

Review

Review: The Metal Additive-Manufacturing Technology of the Ultrasonic-Assisted Wire-and-Arc Additive-Manufacturing Process

Yang Cao *, Yanchao Zhang, Wuyi Ming, Wenbin He and Jun Ma

Mechanical and Electrical Engineering Institute, Zhengzhou University of Light Industry, Zhengzhou 450002, China

* Correspondence: 2015063@zzuli.edu.cn

Abstract: Ultrasonic-assisted wire-arc additive manufacturing (WAAM) can refine microstructures, enhancing performance and improving stress concentration and anisotropy. It has important application prospects in aerospace, weaponry, energy, transportation, and other frontier fields. However, the process parameters of ultrasonic treatment as an auxiliary technology in the WAAM process still have an important impact on product performance indicators, such as the amplitude of the ultrasonic tool, the distance between the points of action of the product, and the scanning speed. The number of ultrasonic impacts influences the performance indexes. Therefore, these parameters must be optimized. This paper describes the advantages and the defects of WAAM components, as well as the principle and development status of ultrasonic treatment technology. Subsequently, this paper also briefly describes how ultrasonic-assisted technology can refine the crystal and improve the mechanical properties of WAAM components. Finally, we review the influence of process parameters (such as ultrasonic amplitude, application direction, and impact times) on the product materials. In this paper, a comprehensive optimization method for ultrasonic parameters is proposed to improve the mechanical properties of WAAM components.

Keywords: metal additive manufacture; wire-and-arc additive manufacture; ultrasonic assistance; mechanical properties; anisotropy; process parameters



Citation: Cao, Y.; Zhang, Y.; Ming, W.; He, W.; Ma, J. Review: The Metal Additive-Manufacturing Technology of the Ultrasonic-Assisted Wire-and-Arc Additive-Manufacturing Process. *Metals* **2023**, *13*, 398. <https://doi.org/10.3390/met13020398>

Academic Editor: Riccardo Casati

Received: 30 December 2022

Revised: 3 February 2023

Accepted: 13 February 2023

Published: 15 February 2023



Copyright: © 2023 by the authors. Licensee MDPI, Basel, Switzerland. This article is an open access article distributed under the terms and conditions of the Creative Commons Attribution (CC BY) license (<https://creativecommons.org/licenses/by/4.0/>).

1. Introduction

With the rapid development of aerospace, shipbuilding, automobile, and rapid manufacturing of molds, modern equipment manufacturing has developed a lightweight, complex structure, few parts, a poor service environment, and high-performance requirements, which result in higher requirements for the accuracy, cost, and manufacturing cycle of such parts. However, it is difficult for traditional casting, forging, and machining methods to meet the manufacturing needs. Thus, there is an urgent need to adopt advanced production technologies to overcome the limitations of traditional molding and manufacturing methods [1–3]. With a high degree of freedom and flexible manufacturing, additive manufacturing (AM) is suitable for the low-cost, small-batch production and manufacture of complex structural and functional parts, especially in the direct forming of metal parts [4]. AM technology involves computer-aided design (CAD). A digital model of the component is discretized into points, lines, or surfaces. It then accumulates the material layer-by-layer to form the 3D model, so that the forming process is highly flexible, and the entire manufacture of mechanical parts or models with a complex structure can be realized without any tools or molds. This layer-by-layer manufacturing feature increases the free degree of design and manufacturing flexibility and can realize complex structure customization and rapid manufacturing and shorten the manufacturing cycle. Compared with traditional manufacturing methods, AM is a “bottom-up” material accumulation manufacturing technology [5–9]. It has been widely recognized and adopted by advanced

manufacturing powers worldwide and has gradually become a research hotspot worldwide [10]. Per ISO/ASTM standards, AM divides the techniques used to create the layers into seven categories, of which the first four on the list are suitable for metals.

1. Binder jetting;
2. Directed energy deposition;
3. Powder bed fusion;
4. Sheet lamination;
5. Material extrusion;
6. Material jetting;
7. Vat photo polymerization.

The directed energy deposition (DED) process is defined as the “additive manufacturing process in which focused thermal energy is used to fuse materials by melting as they are being deposited” per the ISO/ASTM 52900 standard [11,12]. According to the type of heat source, DED technology can be divided into three categories: laser, electron beam, and arc [13–17]. Over the past 20 years, the research has mainly centered on powder-based metal-additive manufacturing that uses laser and electron beams as a source of heat, in which complex structural parts are constantly prepared layer-by-layer through continuous melting or sintering of metal powder. This process has been used in key components of aerospace, defense, military, energy, and other high-tech areas. The additive-manufacturing process of metal includes a complex physical metallurgical process, and the material melting, solidification, and cooling experienced during part forming are all carried out quickly. The solidification process has the common characteristics of a high-temperature gradient, high cooling rate, and local remelting of deposited materials induced by a complex thermal cycle. However, because of the characteristics of its raw materials and heat sources, metal-powder-based laser and electron-beam additive-manufacturing technology is limited to specific structures or components and cannot be formed. Even if it could be formed, the cost of raw materials and time would also be high, and the technology would have many shortcomings, such as: (1) a slow forming rate for the laser heat source and the low laser absorption rate of the aluminum alloy, (2) the vacuum furnace size for the electron-beam heat source being limited to the component volume, and (3) the high cost of the integral forming equipment of the laser heat source and electron-beam heat source [18–22].

As shown in Figure 1, DED technologies include processes with a wire feed and processes with a powder feed. The ability to use yarn as a raw material instead of powder reduces the price per kilogram, increases the efficiency of material utilization, reduces the need for powder recycling systems, creates an environmentally friendly process, and adds the possibility of easy material handling by the operator without health and safety concerns [23]. The most typical example is WAAM. WAAM uses a low-cost arc as the heat source and inert gas as protection; it can be processed in an open environment, and the size of the component is not limited, so the arc-increasing technology has a low manufacturing cost and high processing efficiency. The size of the processing components can be large, so it is especially suitable for metal parts with large-scale complex sizes [24,25].

However, when examining the possibilities and limitations of these methods, it was concluded that additive processes for metal fabrication have many challenges to overcome. In terms of forming morphology, the arc fuse component has the characteristics of large surface roughness and low dimensional accuracy. In the microstructure, the arc fuse component has the characteristics of a rough structure, directed growth, and separation of the composition. In terms of mechanical properties, the arc fuse component has the characteristics of significant anisotropy and heterogeneity. There are many process parameters of WAAM that greatly influence the above characteristics of the product [26–28]. To address these problems, many universities and research institutions have initiated relevant research and proposed various interlaminar strengthening processes and processing methods, such as laser impact peening, mechanical hammering, interlayer rolling, ultrasonic impact, ultrasonic vibration, and micro-forging strengthening technologies [29]. These technologies can effectively reduce the residual stress, thermal deformation, porosity, and surface rough-

ness of the deposited parts. At the same time, the directed growth of the microstructure caused by the temperature gradient of the metal parts is improved, and the coarse column crystalline structure transforms into a fine equiaxed crystal structure. Then, the grain refinement and homogenization of the microstructure distribution are obtained, which can improve the microhardness and tensile properties of the parts and reduce the degree of anisotropy [30–34]. The ultrasonic vibration interlayer-strengthening technology is based on controlling the solidification process of the molten pool to refine the microstructure and achieve the purpose of strengthening. The means of laser impact, mechanical hammering, inter-laminar rolling, and micro-forging interlayer strengthening mainly rely on the plastic deformation on the surface of the deposition layer, and the dislocation wall is formed after a large number of dislocations are multiplied and then transformed into sub-grains to realize grain refinement. In addition, plastic deformation greatly increases the deformation energy storage in the treatment area. Promoting recrystallization under the comprehensive thermal effect of the subsequent deposition layer can effectively change the internal structure of the parts, weaken or even eliminate the anisotropy, and improve the overall properties. Among these post-processing technologies, ultrasonic-assisted manufacturing is the mainstream method for products at present. Ultrasonic-assisted manufacturing includes the technology of ultrasonic impact and ultrasonic vibration. The treatment process and equipment are relatively simple but can greatly improve the properties of the products, which has broad research and application prospects in AM [35–42]. Wang et al. [43] reduced several problems (e.g., heterogeneous microstructures, internal cavities, and large porosity) that exist in laser-engineered net-shaping (LENS)-fabricated IN718 parts. Ultrasonic vibration-assisted (UV-A) LENS was developed based on the ultrasonic vibration's actions in material melting and solidification. This process is an effective manufacturing method in the fabrication of IN718 parts.

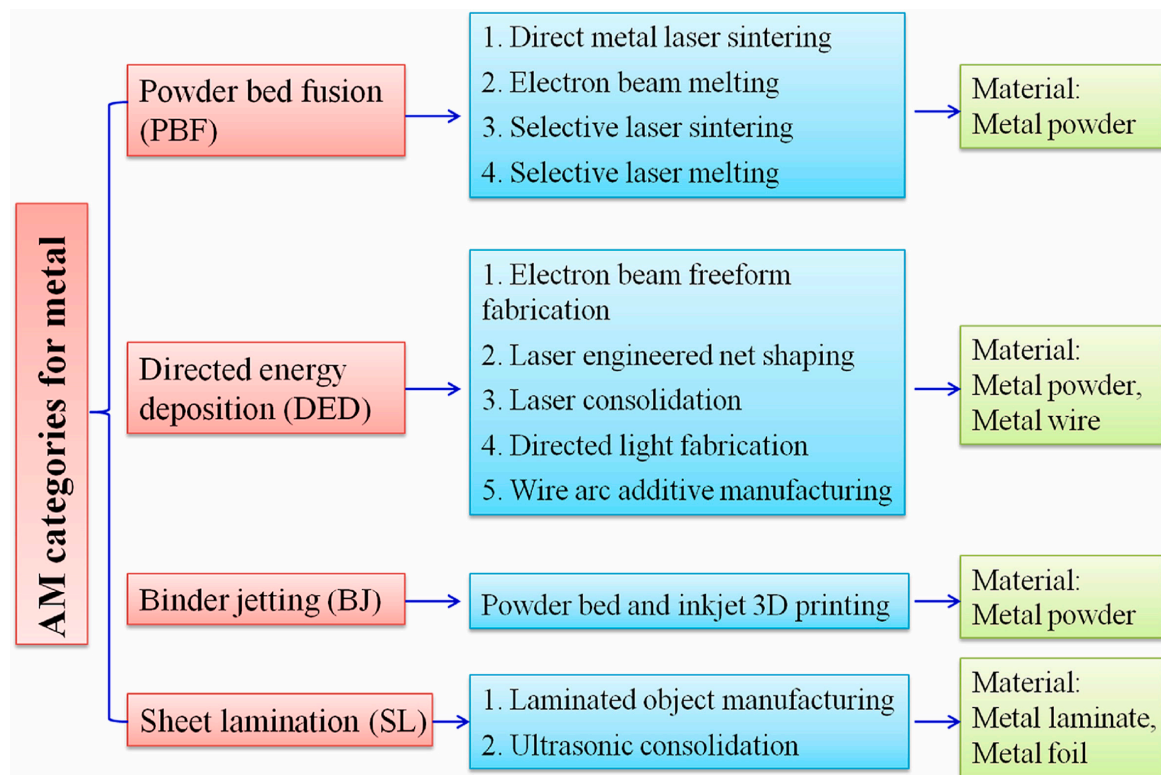


Figure 1. Classification of metal additive manufacturing, reproduced or adapted from [13], with permission from Elsevier, 2021.

At present, the research on ultrasonic-assisted additive manufacturing generally investigates the effect of ultrasonic vibration on the microstructure and mechanical properties of additively manufactured parts under the conditions of a single parameter, and there are a few studies on the effect of ultrasonic multi-parameter optimization. Based on this situation, this paper briefly introduces the advantages of WAAM and the unavoidable shortcomings of the WAAM workpiece, summarizes the development status and existing problems of ultrasonic-assisted technology, and discusses the characteristics and advantages of ultrasonic-assisted WAAM. Finally, the ultrasonic-assisted process parameters are analyzed in detail. A comprehensive optimization method for ultrasonic parameters is proposed to improve the mechanical properties of WAAM components, which can lay the foundation for the application of wire-arc manufacturing components in the aerospace field and forecast the development trend.

2. Introduction of Wire-Arc Additive Manufacturing

WAAM is an advanced material-increasing manufacturing technology [44] that uses the arc as the heat source and the wire as the raw material. The melted wire is deposited layer-by-layer under the control of the program. According to the established three-dimensional digital model, the metal parts are gradually formed by line to the surface and then to the body. Because it uses fewer materials for the manufacturing of components than other AM techniques, WAAM has proven useful in terms of consumption, and the equipment cost is comparatively low. In general terms, a comparison of the main characteristics of AM technologies is shown in Table 1. A schematic diagram of WAAM is shown in Figure 2.

Table 1. Comparison of main metal additive-manufacturing processes [45].

Factors	PBF	LMD	EBAM	WAAM
Accuracy	High: $\pm 0.05\text{--}0.2$ mm	Mean: ± 0.2 mm	Requires final machining	Requires final machining
Structural integrity	High: vacuum chamber/protected atmosphere	High: protected atmosphere	High: empty chamber	High: protected Atmosphere
Productivity	Low: $\sim 0.1\text{--}0.2$ kg/h Limited by working space (max. $800 \times 400 \times 500$ mm)	Average: $\sim 0.5\text{--}1$ kg/h	High: $3\text{--}11$ kg/h	High: ~ 10 kg/h
Part size		Large, limited by machine range	Large, limited by machine range	Large, limited by the range of the machine
Geometric complexity	High	Media	Low-medium	Low-medium
Industrial application	Direct manufacture of complex parts	Repair of parts, coatings, direct	Repair of parts, coatings, direct	Repair of parts, coatings, direct
Price of equipment	High	High	High	Under
Raw material cost	Very High	High	Under	Under

2.1. Characteristics of Wire-Arc Additive Manufacturing

WAAM can be used to manufacture large components because of its high deposition efficiency, low deposition cost, and high material utilization. The high flexibility of WAAM equipment can realize the deposition of metal parts with different shapes [46]. Furthermore, more traditional processes can be combined with the technology to solve the problems of coarse microstructure and the low mechanical properties caused by the large heat input to further improve the comprehensive mechanical properties of deposited materials.

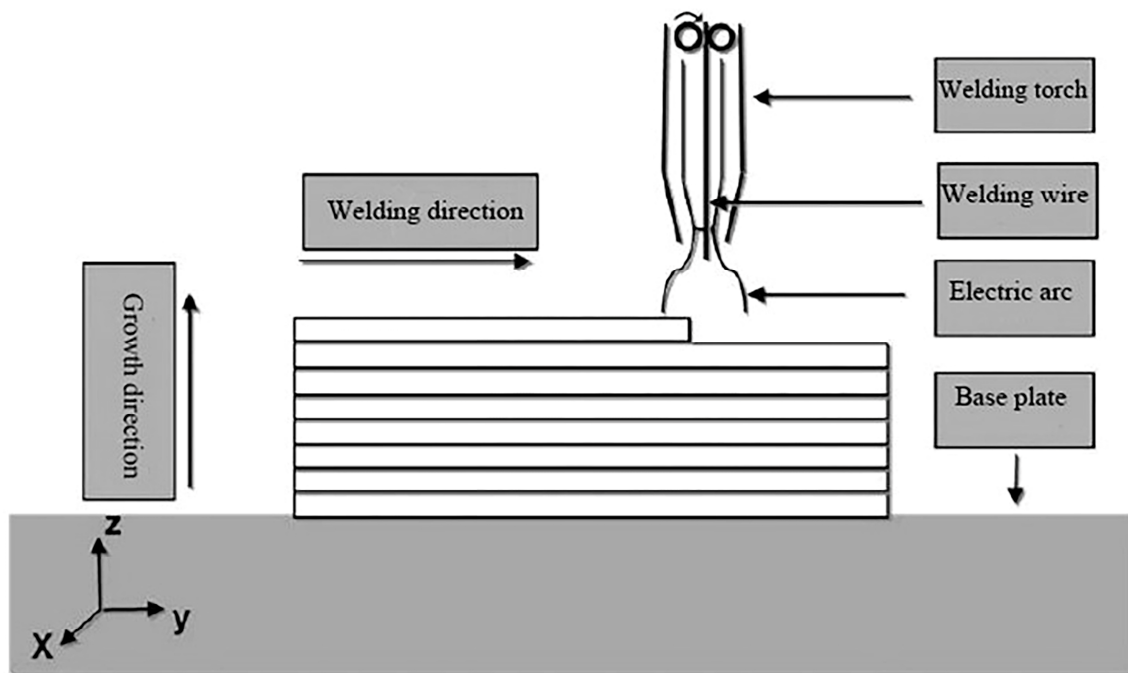


Figure 2. Schematic diagram of wire-arc additive-manufacturing principle.

(1) The material utilization and manufacturing efficiency

The high material utilization rate of WAAM is one of its most important benefits for the aerospace industry. Martina et al. [47] formed a Ti-6Al-4V thin-walled wall by WAAM and determined its process window. They found that the stacking width of the thin-walled wall can reach 17.4 mm, the material utilization rate can reach 93%, and the deposition rate can reach 1.8 kg/h.

(2) The size of the product

In the laser- and electron-beam additive-manufacturing technology, the forming size of the product is limited by the forming chamber, powder bed, and electron-beam vacuum chamber, which is a bottleneck in its development. WAAM does not require strict atmosphere protection, and the size of the product and forming equipment is almost unlimited, which effectively solves the forming size problems of laser and electron-beam additive manufacturing [48].

(3) The composition and high compactness of the product

There are many defects in the forming process of laser-forming metal powder technology, such as porosity and unfused components. WAAM has a long high-temperature arc time and a large molten pool. Therefore, the components have uniform composition and high compactness. Compared with ingot metallurgy, the mechanical properties and overall quality of the component are better and have the characteristics of high toughness, high heat treatment stability, and high thermal fatigue cracking resistance [49–51].

2.2. Defects in the WAAM

After years of development, the performance of the WAAM process has been significantly improved. However, in the preparation process, the materials easily produce defects such as micro-pores, micro-cracks, and deformation. The reasons may include improper setting of welding parameters, low precision of the welding machine, unstable wire transportation, welding heat accumulation, and the manufacturing environment. As shown in Table 2 [52], there are many forms of processing: Gas Metal Arc Welding (GMAW), Gas Tungsten Arc Welding (GTAW), Tungsten Inert-Gas (TIG), Cold Metal Transfer (CMT), Direct Current Electrode Positive-GMAW(DCEP-GMAW), Double-electrode gas metal

arc welding (DE-GMAW), Variable-polarity gas metal arc welding (VP-GMAW), CMT pulse advanced (CMT-PADV), Pulsed plasma arc deposition (PPAD), Pulse metal inert gas (PMIG).

Table 2. Defects in WAAM [52].

Material	Welding Process	Defect Type					
		Porosity	Crack	Deformation	Anisotropy	Substrate Adherence	Surface Quality
Ti-6AL-4V	TIG	-	-	-	Serious	Good	Good
	Plasma	-	-	-	Light	Good	Good
	CMT	-	-	-	Serious	Good	Good
	DCEP-GMAW	-	-	-	Light	Medium	Poor
HO8Mn2Si steel	DE-GMAW	Low	-	-	Light	Good	Medium
Copper-coated steel	GMAW	-	-	-	Light	Good	Medium
ER4043 aluminum alloy	CMT	High	-	-	Light	Good	Good
	VP-GMAW	-	-	-	Light	Good	Medium
AA2319 aluminum alloy	CMT	High	-	-	Light	Good	Good
	CMT-PADV	-	-	-	Light	Good	Good
5356 aluminum alloy	VP-GMAW	-	✓	-	Light	Good	Good
Inconel-625	PPAD	High	✓	-	Light	Good	Good
	GTAW	-	-	-	Light	Good	Good
Inconel-718	GMAW	High	✓	✓	Light	Good	Good
AZ31 magnesium alloy	PMIG	-	-	-	Serious	Medium	Medium
Nickel–aluminum–copper	CMT	-	-	-	Light	Good	Good
Steel-bronze bimetal	GMAW	-	-	-	Light	Good	Good

Researchers have analyzed the microstructure and properties of WAAM products and found that the mechanical properties were reduced. Taking pores and residual stress as examples, the disadvantages of the materials caused by the defects in the WAAM process are briefly described.

(1) Porosity

As one of the main defects in metal additive manufacturing, porosity defects seriously affect the quality of manufacturing workpieces. Effective control and elimination of stomata is the key technology for improving the quality of the product in AM. Kobayashi et al. studied the cast alloy Al-Si-Mg [53], and they found that the porosity seriously affects the degree of the error. Because of the reduction in the tensile bearing capacity of the pore zone, the pore zone yields first, resulting in strain concentration near the pore and thus premature fracture. The study result suggested that the elimination of pores in aluminum is crucial to improving its mechanical properties. Yi et al. [54] welded 6061 aluminum alloy T-joints using a double pulse MIG welding process. Then, the welded T-joints were post-weld heat-treated. The microstructure of the weld with different aging temperatures and times was studied by transmission electron microscopy and scanning electron microscopy. The mechanical properties were tested by a hardness test and tensile test. They found that the aluminum alloy easily produces pores and voids in the WAAM process because of the high thermal expansion coefficient, high solidification shrinkage, and other welding characteristics of aluminum alloy. The high melting point dense oxide film (alumina) is easily formed on the alloy surface, and the molten metal is blocked in the molten pool, which prevents the metal from being deposited.

In order to control pores, most scholars considered the cleanliness of raw materials themselves, thereby reducing porosity at the source. If there is a degree of contamination,

such as water, grease, or other hydrocarbons, on the surface of the wire or substrate, it is difficult to remove, and these pollutants can be easily absorbed by the molten pool and then produce pores after solidification.

(2) Residual stress and deformation

Because of the large heat input of arc fuse technology and the complex temperature-field distribution of the workpiece, the deformation and residual stress produced by this process are inevitable. In the WAAM of titanium alloys, Zhang et al. [55] found that the existence of welding residual stress at the interface causes microscopic deformation of the parts, including longitudinal and transverse thermal shrinkage, bending deformation, shear deformation, and torsion deformation. Chi et al. [56] studied the microstructure of metals manufactured by WAAM technology and found that there were many columnar grains that created harmful residual tensile stress in the product. After heat treatment and laser impact strengthening, serious plastic deformation occurred on the surface of the product. The plastic deformation transformed the residual tensile stress into compressive stress, which was beneficial to the product. Malcolm Dinovitzer et al. [57] used 304 stainless-steel plates as the substrate for WAAM technology. They used the Taguchi method and analysis of variance (ANOVA) to determine the travel speed, wire feed rate, current, and argon flow rate. They found that increasing travel speed or decreasing current caused a decrease in melt-through depth and an increase in roughness. Fernando Veiga et al. [58] applied WAAM to Invar. They utilized and unified research material previously investigated in WAAM technology and took a new approach based on the study of symmetrical phenomena that guarantee the quality of the process. On the other hand, the monitoring of the symmetry of the melting pool utilized thermography techniques. The geometry of the zero beads was determined through the analysis of the coefficient of symmetry in the longitudinal and transverse planes. The results indicated that residual stress and deformation are generated in the process of WAAM.

3. The Current Status of Ultrasound-Assisted Development

Ultrasonic-assisted additive manufacturing mainly includes ultrasonic vibration technology and ultrasonic impact treatment (UIT). The two methods can be traced back to the 1960s, beginning with the research of Mukhanov et al. [59]. The researchers applied the continuous output ultrasonic vibration produced by the ultrasonic transducer directly on the surface of treated hard materials such as carbide alloy and rhinestone. A thin plastic deformation layer was formed on the surface of the treated material, and the microstructure and the residual stress distribution of the deformation were changed. In the 1970s, Statnikov formally proposed the UIT technology [60]. In recent years, ultrasonic assistance as a post-processing technology has been widely studied.

3.1. Ultrasonic Vibration-Assisted Technology

The ultrasonic vibration system consists of an adjustable height frame, generator, transducer, and tool head. First, the ultrasonic generator converts ordinary alternating current into ultrasonic-frequency alternating current, then the ultrasonic-frequency alternating current is converted into mechanical vibration with the same frequency by the transducer. The mechanical vibration then acts on the tool head through the horn; under the effect of self-weight and external pressure, the tool head applies high-frequency vibration to the corresponding working parts, such as the welding platform, weld, or corresponding experimental parts, to improve the material performance [61].

When the high-power ultrasonic wave propagates in the liquid metal, the mechanical, thermal, cavitation, and sound flow effects are produced by the high-frequency vibration, which can refine the grain and homogenize and purify the structure, for example by degassing, slag removal, and purification [62]. Some scholars have introduced ultrasonic vibration technology into the AM process to improve the microstructure and reduce residual stress. Cong et al. [63] studied a novel ultrasonic vibration-assisted laser-engineered net-shaping (LENS) technology. They found that the introduction of ultrasonic vibration

energy into the molten pool in the LENS process can reduce the voids and microcracks and significantly refine the grains of the deposited samples. Chen et al. [64,65] studied the effect of ultrasonic vibration on the laser cladding process. The results indicated that ultrasonic vibration can reduce cracks, homogenize chemical composition, refine the microstructure, and improve the properties of the cladding layer. Qin et al. [66] investigated the process of ultrasound-assisted laser deposition of a titanium alloy. They suggested that the solid crystal network formed by the staggered connection of primary dendrites is broken by the ultrasonic cavitation and mechanical effect, and the grains are refined. At the same time, the melt is supplemented during continuous crystallization, and the tensile stress between dendrites is reduced. Wang [67,68] discussed the microstructure and properties of IN718 deposited by ultrasonic vibration-assisted laser forming. The results indicated that the surface roughness and residual stress of the parts were significantly improved after ultrasonic vibration. The microstructure, tensile, and yield strength were remarkably improved. Yashwan et al. [69] welded a 6061-T6 aluminum alloy to a 6082-T6 aluminum alloy of a different thickness. The joint was prepared by an ultrasonic-assisted cold metal transfer (U-CMT) welding process, and the mechanical properties and microstructure of the joint were improved. The results revealed that the weld-bead dimensions were increased with the aid of ultrasonic vibrations. The tensile strength and microhardness of the welding joint were enhanced. Yuan of Harbin Engineering University [70] proposed a manufacturing method for the metal additive by introducing ultrasonic vibration in the laser-fuse additive process and studied the microstructure evolution of a titanium alloy in this process with a high-power ultrasonic energy field. The ultrasonic vibration device in this study adopted an innovative structural design, and the amplitude transformer and ultrasonic probe were rigidly connected to maintain better wear resistance and toughness of the device, as shown in Figure 3. The ultrasonic wave acts on the molten pool at ultrasonic frequency (20 kHz), resulting in sound pressure and cavitation in the molten pool, which effectively restrains the epitaxial growth trend of the primary β crystal of the titanium alloy, refines the grain structure of the titanium alloy, and promotes the formation of the equiaxed crystal. According to the above analysis, the introduction of ultrasonic vibration energy improved the internal structure of the material, made the microstructure of the deposition layer more uniform and the grain finer, and at the same time effectively reduced the residual stress in the material.

3.2. Ultrasonic Impact Treatment Technology

In the UIT technology [71,72] electrical oscillation signals with high frequency in the 15~40 kHz range are output by the ultrasonic generator and then transformed into a high-frequency mechanical vibration by the transducer. The amplitude of the mechanical vibration is amplified and transmitted to the vibrating tool head by the horn connected to the transducer, which promotes the high-frequency impact movement of the impact needle in the impact gun, and the projectile hits the part surface to strengthen it. Figure 4 contains a schematic diagram of the UIT process.

The equipment used in this technology has the advantages of small size, easy operation, and high energy density input, so it is widely used in the welding industry. The UIT process can eliminate the residual tensile stress of welded joints, introduce beneficial compressive stress, reduce the stress concentration on the surface of welded joints, and improve the fatigue performance of welded joints [73,74]. Roy et al. [75] tested the fatigue resistance of welded transverse stiffeners and cover plate details by UIT and determined the residual stress distribution near the weld toe before and after treatment. The results indicated that UIT can smooth the profile of the weld toe, improve its microstructure, and introduce beneficial compressive residual stress in the weld area. Mordyuk et al. [76] studied the effect of UIT on the forming process of AISI 321 stainless steel and found that the nanocrystalline surface layer was formed after UIT. Yang et al. [77] studied the UIT-assisted WAAM-forming Ti-6Al-4V alloy. The results revealed that most of the residual stress was eliminated, and a refined bamboo-like microstructure was formed in the process; the grain size of this

bamboo-like structure was much smaller than the coarse columnar grains. Cheng et al. [78] investigated the influence of ultrasonic impact treatment on austenitic stainless-steel welds. The residual stress test results showed that the residual compressive stress was produced in the ultrasonic impact area at a depth of 1.5~1.7 mm and a width of 15 mm. The maximum compressive stress of the treated materials exceeded the yield strength of the base metal. Rao et al. [79] took Q345 steel as the research object to analyze the effect of ultrasonic impact on weld residual stress. The stress measured by the hole-drilling technique was reduced by 34~55% at the weld depth of 2~4 mm under ultrasonic impact conditions. Mordyuk et al. [80] analyzed the microstructure changes of Zr-1%Nb alloy after ultrasonic vibration treatment for 4 min. The results showed that an ultra-fine grain formed on the surface of the Zr-1%Nb alloy, and the grain size was about 100 nm. In the abovementioned studies, UIT technology was shown to significantly reduce the residual stress in the material and improve the internal structure.

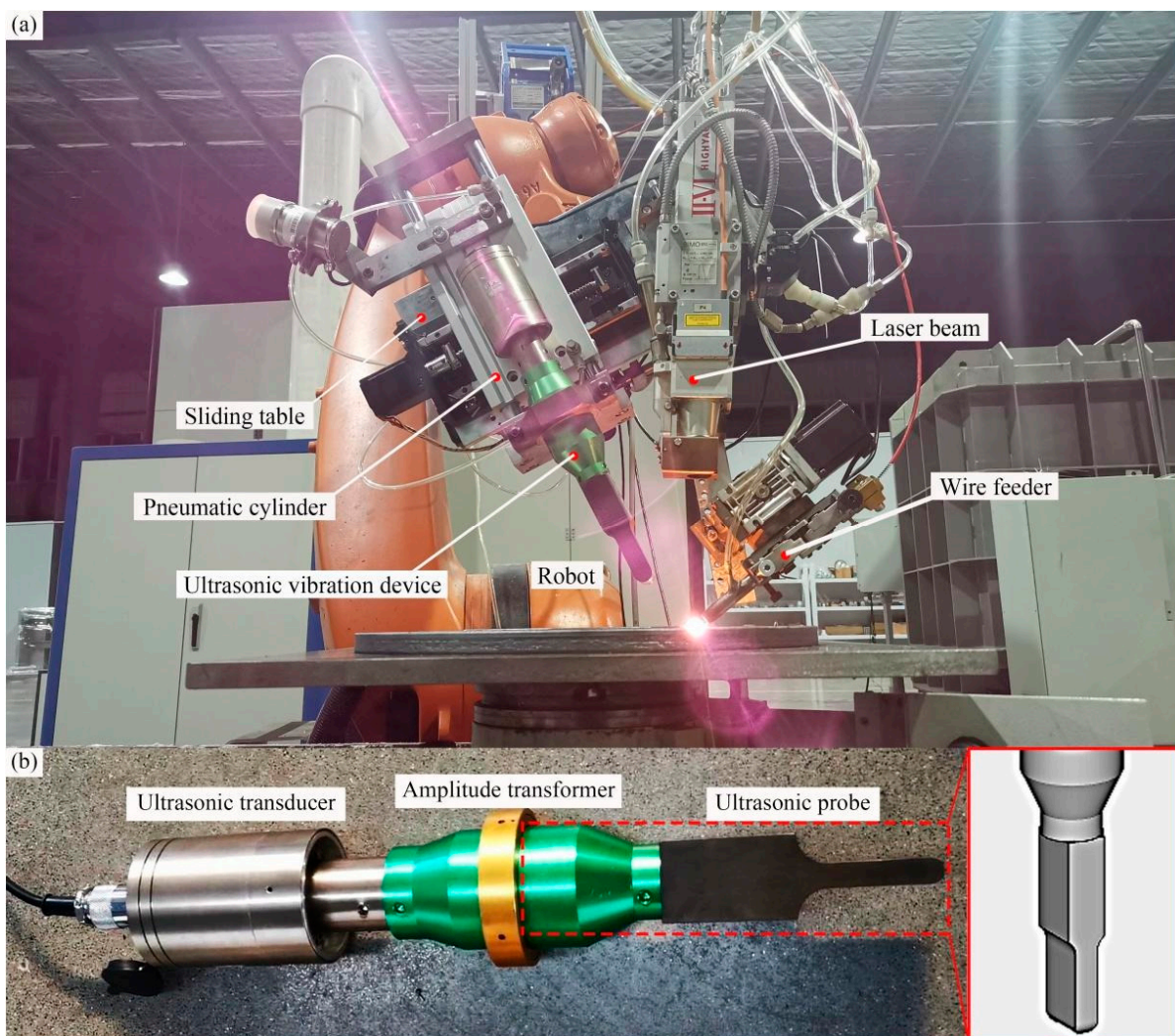


Figure 3. Set-up for LWAM assisted with ultrasonic vibration: (a) overall arrangement diagram; (b) an ultrasonic vibration device, reproduced or adapted from [70], with permission from Elsevier, 2021.

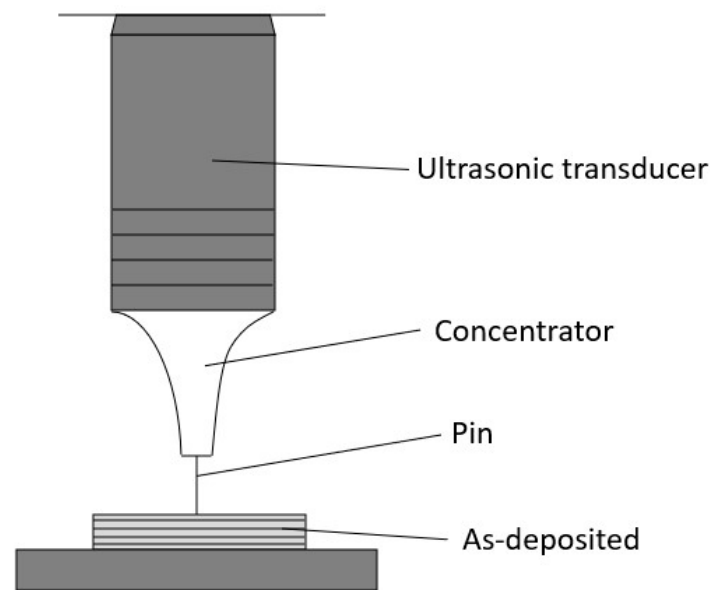


Figure 4. Schematic diagram of the UIT process.

4. UIT-Assisted WAAM

There is a complex physical metallurgical process for the metal parts during the arc fuse forming process. The as-cast microstructure is presented in the materials with the high temperature of the welding heating source, resulting in a dendritic structure, coarse grains, and so on. These problems significantly affect the mechanical properties, such as toughness, strength, and fatigue properties, and cause the anisotropy of the material. To solve these problems, UIT technology was introduced as a post-processing method to improve the synthesized material properties [81].

Figure 5 shows a schematic diagram of UIT-assisted WAAM equipment. The ultrasonic generator is connected to the welding head of the gas metal arc-adding manufacturing (GMA-AM) equipment through the two fixtures. In the process of adding material, the impact thimble is aligned and perpendicular to the deposition layer so that it impacts the deposition surface by self-weight after the movement of the robot [82].

4.1. Ultrasonic-Assisted Elimination of Residual Stress

When the weld toe is subjected to ultrasonic impact treatment, the smooth transition at the weld toe is realized, the stress concentration factor is reduced, and the residual tensile stress is reduced or even eliminated, and it is possible to introduce residual compressive stress. As a result, the mechanical properties such as the tension and fatigue of the weld can be improved [83].

Cheng et al. [78] explored the internal stress of ultrasonic impact and shot peening by neutron diffraction and X-ray diffraction and measured the residual stress under ultrasonic impact conditions for the first time. They found that the compressive stress produced by the two techniques was greater than the yield stress of the matrix material, and the compressive stress caused by the ultrasonic impact was about 1.6 mm, while the depth of the stress layer produced by shot peening was about 0.8 mm. Ye of the Armored Army Engineering College and others studied the effect of ultrasonic impact on the residual stress and fatigue performance of ultra-high-strength steel welded joints and tested the solder joint and weld bead with an X-ray stress analyzer [84]. They found that the fatigue strength of the welded state increased by 33.3% after ultrasonic impact treatment. Amir Abdullah et al. [85] studied the effect of UIT on the residual stress of 304 stainless-steel welded joints. UIT reduced the stress concentration factor at the weld and increased the fatigue life of the components by 29%. Xiao used the method of real-time ultrasonic impact to eliminate the residual stress of the sample and carried out an ANSYS simulation [86]. It was found that the real-time ultrasonic impact on the back of the weld effectively improved

the longitudinal residual stress, but the improvement of the transverse residual stress was not obvious. The surfacing on a 10 mm-thick plate produced the stress of 39.36 MPa transversely and 210 MPa longitudinally. After real-time UIT, the longitudinal residual stress was eliminated by about 33.38%. When Gao used the ultrasonic impact to treat the multi-layer welding of high-strength alloy steel [87], it was found that ultrasonic impact could significantly improve the residual stress of multi-layer welding parts. The maximum tensile stress after impact was about 28% lower than that during welding.

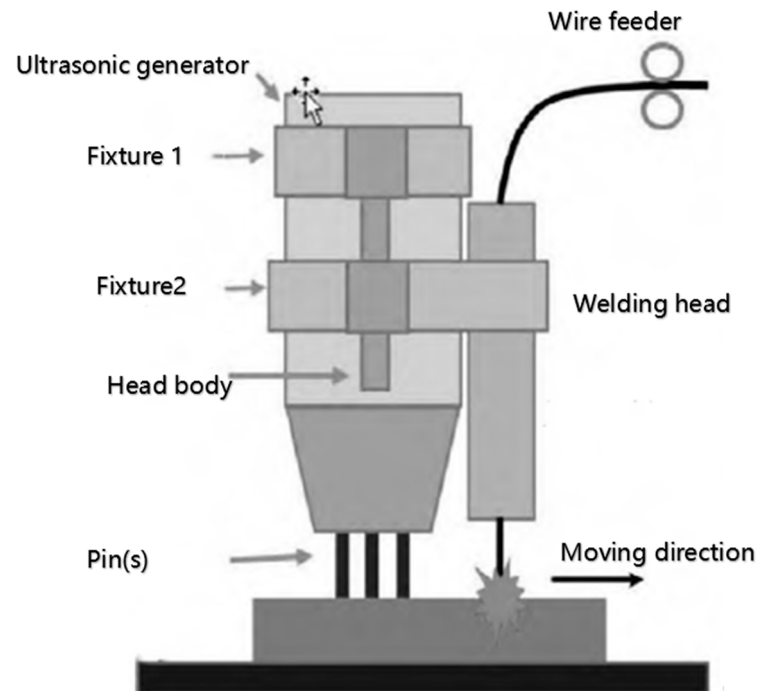


Figure 5. Schematic diagram of joint equipment.

4.2. Ultrasound-Assisted Preparation of Nano-Layer on Metal Surface

Ultrasound-assisted additive manufacturing can help the metal surface to obtain nano-layers, and nanomaterials have excellent mechanical and physical properties because of their unique structure. Preparing a nano-layer on the metal surface can optimize the comprehensive mechanical properties and service environment of the materials.

Shao et al. [88] studied the effect of different levels of ultrasonic power on the grain refinement of the AZ80 alloy. Table 3 shows that ultrasonic impact can refine grains. From 0 to 600 W, the average grain size decreased from 387 to 147 μm . However, when the power increased from 950 to 1400 W, the average grain size increased. The thermal effect of ultrasound may be an important reason for this transformation.

Table 3. Effect of ultrasonic power on the grain size of the AZ80 [88].

Ultrasonic power/W	0	200	400	600	800	1000	1400
Average grain size/ μm	387	199	175	147	168	184	207

Wang et al. [89] studied the ultrasonic impact treatment of 4Si steel. Through ultrasonic surface nano-processing, the working head exerts a certain degree of ultrasonic-frequency mechanical vibration on the workpiece along the normal direction of the surface, and under the conditions of a certain static pressure and feed speed, the working head transmits the pressure and ultrasonic impact vibration to the surface of the machined machinery parts in the rotating state, and the material produces elastic-plastic deformation by ultrasonic punching. A nano-layer was obtained on the surface, and the average grain size was about

50 nm. Hu of Qingdao University of Technology (Qingdao, China) and others emitted ultrasonic vibration to the surface of the molten pool through an ultrasonic horn installed on the side axis [90], thus exerting an influence on the laser cladding process. They found that the ultrasonic flow accelerated the flow of the molten pool and suppressed the element segregation. Xu et al. [91] of Jiangsu University introduced ultrasound to assist laser cladding to prepare an iron-based coating by means of substrate vibration. They found that the original columnar crystal in the coating was transformed into the fine equiaxed crystal, and the hardness, elastic modulus, and wear resistance of the coating were improved. Wen of Harbin Engineering University fabricated the AlCrCoFeMn_{0.5}Mo_{0.1} coating by introducing ultrasound into the substrate vibration to assist laser cladding [92]. It was found that the dilution rate of the coating increased with the increase in laser line energy.

4.3. Ultrasound-Assisted Improvement of Morphology

To improve the morphology of the weld-toe zone through the study of the titanium alloy butt joint and cross joint after UIT, Yang and others [93] found that relative to the transition radius of the weld-toe zone, there is no obvious change in weld height, width, or inclination angle. The stress concentration factor decreases with the increase in the weld-toe transition radius. After UIT, the stress concentration factor of the butt joint and cross joint is reduced by 20% and 22%, respectively. Zhao of Tianjin University (Tianjin, China) and others [94] studied the fatigue properties of TC4 welded joints and calculated the stress concentration factor by ANSYS. They found that the stress concentration factor at the weld toe was 4.1. After ultrasonic impact, the stress concentration factor decreased to 2.79. The geometry of the weld toe was improved, and the stress concentration degree was improved by about 47%.

4.4. Ultrasonic-Assisted Improvement of Fatigue Strength

Per Jahn Haagensen et al. [95] evaluated the ultrasonic impact on high-strength steel and welded AA5083 aluminum plates and found that the ultrasonic impact can greatly improve the fatigue prosperities of samples, in which the fatigue strength of an aluminum alloy and high-strength steel increased by 93% and 121%, respectively. Based on the finite element simulation of ductile damage of GTN, Yang et al. revealed the plastic damage of AISI304 stainless steel caused by ultrasonic impact technology [96]. In their study, they found that the damaged area of the ultrasonic impact process was annular, and the indentation center was not affected. The main pores in the aluminum alloy WAAM process are hydrogen pores, and hydrogen elements mainly come from the surface of the aluminum substrate, welding wire, and protective gas atmosphere. The effects of ultrasonic frequency on the porosity of the fabricated IN718 parts are shown in Figure 6 [43]. Compared with the LENS process without ultrasonic vibration, UV-A LENS produced reduced pore number and average pore size, as shown in Figure 6a–d. Figure 6e shows that the porosity value first decreased after introducing ultrasonic vibration with a frequency of 25 kHz and then increasing the ultrasonic frequency from 25 to 41 kHz.

4.5. Other Methods

He et al. [97] experimented with arc adding and ultrasonic impact to manufacture titanium alloy parts, and the properties of the parts were optimized by ultrasonic impact. The results indicated that the ultrasonic impact broke the microstructure of the sample from columnar to fine equiaxed grains, and the isotropy of the material increased from 12.5% to 1.5%. Xu et al. [98] studied the effect of ultrasonic vibration on the microstructure and properties of the formed parts in the process of CMT addition to TC4 titanium alloy. The results showed that compared with the parts without ultrasonic vibration, the grain size of the parts formed by ultrasonic vibration was reduced, and the mechanical properties were significantly improved. Chen and others [99] studied the effect of ultrasonic vibration on the microstructure and tensile properties of aluminum bronze alloy made by arc addition. The results indicated that under the ultrasonic impact conditions, the microstructure of the

sample was refined, the tensile strength increased from 436.5 ± 2.1 to 516.1 ± 0.5 MPa, and the anisotropy was effectively restrained. Ding et al. [70] studied the effect of ultrasound on the grain refinement of the Ti-6Al-4V alloy produced by laser fusing. The results showed that the introduction of ultrasonic impact can effectively restrain the epitaxial growth of the β crystal, weaken the texture strength of the β crystal, and refine the microstructure of the formed parts. Figure 7a [100] shows the inverse pole figure (IPF) orientation map of the austenite (face-centered cubic, FCC) phase along the building direction in the deposited layer without UV. It indicates that the grain structure within a 1.0 mm distance from the substrate has extremely irregular morphology, the columnar dendritic grains grow epitaxially along the building direction, and many fine grains exist between the coarse columnar dendritic grains. In contrast, the grain structure of the deposition layer with UV is more uniform, and there are a few large amounts of coarse columnar dendrite grains in the deposition layer (see Figure 7b).

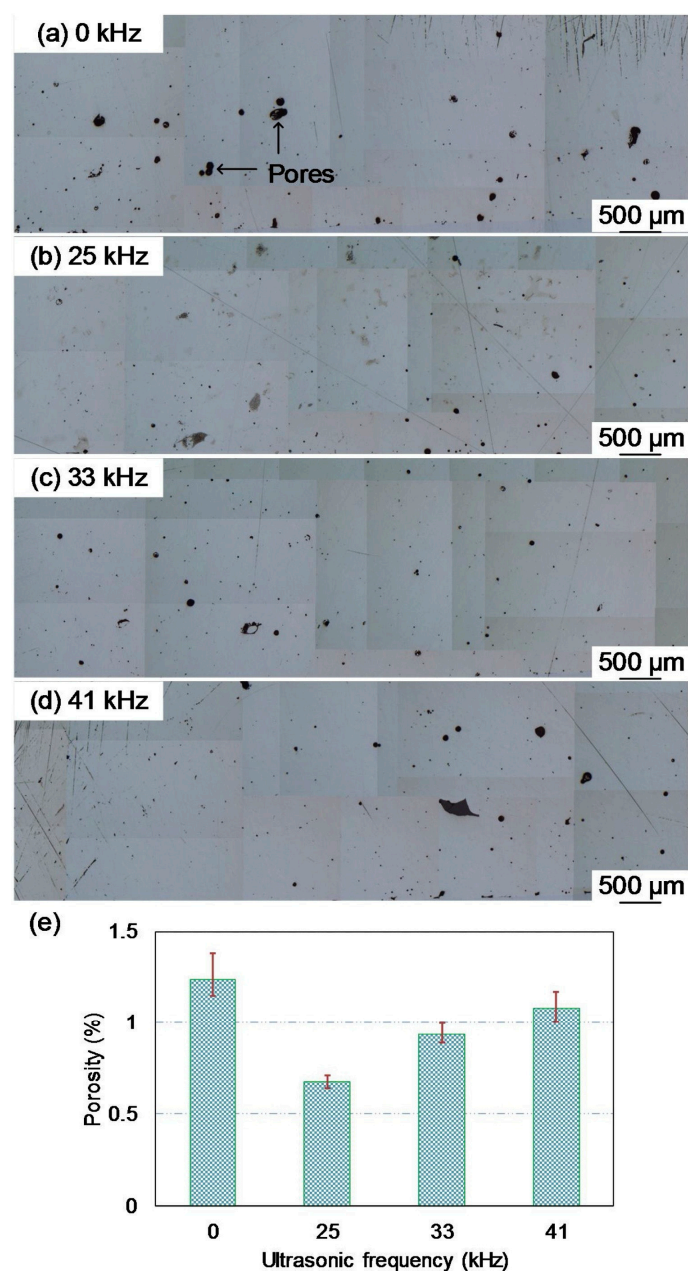


Figure 6. Effects of ultrasonic frequency on porosity: (a) 0; (b) 25; (c) 33; (d) 41 kHz; (e) effects of ultrasonic frequency, reproduced or adapted from [43], with permission from Elsevier, 2020.

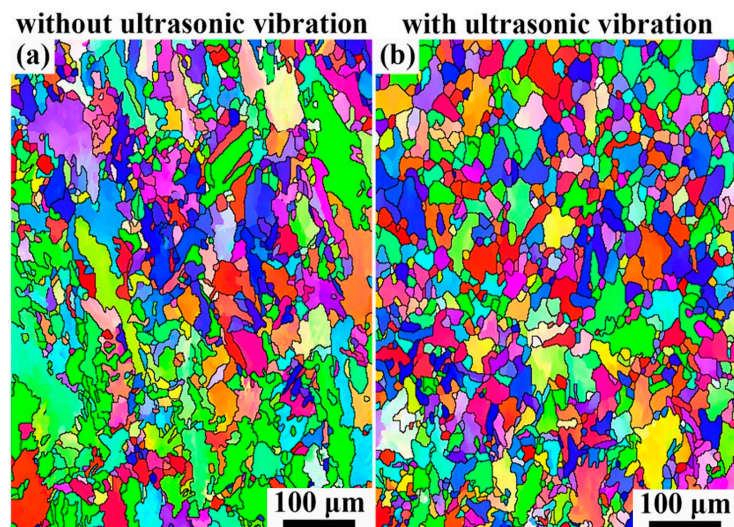


Figure 7. Inverse pole figure (IPF) orientation maps depicting grain structures along the building direction (z) for the austenitic phase in samples: (a) no additional ultrasonic vibration; (b) additional ultrasonic vibration, reproduced or adapted from [100], with permission from Elsevier, 2021.

Through the comparison of Figure 7a,b, it can be seen that the grain structure of the deposited parts is obviously refined after additional ultrasonic vibration.

5. Ultrasound-Assisted Process Parameters

In the process of ultrasonic-assisted WAAM, the amplitude of the ultrasonic tool, the distance between the action points of the product, the scanning speed, and the number of ultrasonic impacts have an important influence on the performance indexes. This section further analyzes and discusses the mechanism of columnar-crystal and strip-band formation and columnar-crystal transformation into the equiaxial crystal and the influence of ultrasonic-assisted treatment process parameters.

5.1. Ultrasonic Amplitude

Ultrasonic amplitude is one of the main parameters of an ultrasonic device. It determines the maximum amplitude of ultrasound acting on the sedimentary layer. After the action spacing is fixed, the difference in the input ultrasonic amplitude also directly determines the intensity of the ultrasonic energy field acting on the molten pool, which determines the influence of ultrasound on the solidification process of the molten pool.

As shown in Figure 8, the surface of sample 1 without ultrasonic vibration is covered with the metallic luster, its weld width is 5 mm, and reinforcement is 4.2 mm. Compared with sample 1, the surface of sample 2 obviously loses the metallic luster and capillary waves appear (it does not affect the formed appearance), its weld width is 5.7 mm, and the reinforcement is 4 mm. A small number of tiny pores appear on the surface of sample 3, and a larger number of pores gather on the surface at the arc-end point. Its weld width is 5.8 mm, and the reinforcement is 4 mm. The phenomenon of the accumulation of pores at the shallow surface of the weld can be explained as follows: With the promotion of the ultrasonic wave, the tiny bubbles escape upward. When the next layer of cladding is carried out, the cladding metal melts the metal below the weld, and most of the pores are eliminated, leaving only some pores farther away from the weld surface. It can be concluded from samples 1, 2, and 3 that the ultrasonic vibration increases the weld width and lowers the reinforcement.

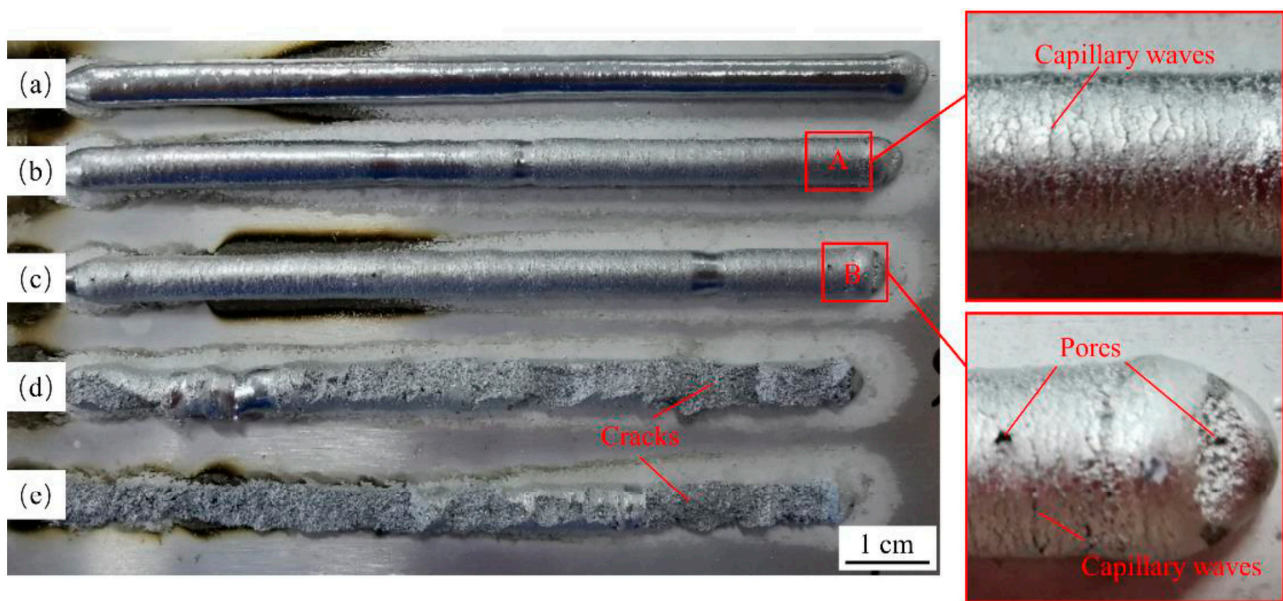


Figure 8. Effect of different ultrasonic amplitudes on weld: (a) sample 1; (b) sample 2; (c) sample 3; (d) sample 4; (e) sample 5, reproduced or adapted from [81], with permission from MDPI, 2022.

As shown in Figure 8d,e, with the increase in ultrasonic amplitude, it can be seen that the incompletely solidified weld cracks because of the excessive energy of ultrasonic vibration. Thus, when the molten pool is not completely solidified, the weld cracks when the tensile stress generated by ultrasonic vibration during the vibration period exceeds the ultimate tensile strength that can be endured in this state.

In other words, in the process of WAAM assisted by ultrasonic vibration, when the distance between the ultrasonic vibration and the molten pool is fixed, only when the input ultrasonic amplitude reaches a certain threshold can it greatly influence the solidification process of the molten pool [101] to meet the needs of microstructure refinement. Through a comparison of the temperature gradient, cooling rate, and solidification rate with different amplitudes, ultrasonic vibration was found to accelerate the flow in the molten pool with the increase in ultrasonic amplitude, thus homogenizing the temperature field, reducing the temperature gradient in the molten pool, and improving the solidification speed of the molten pool [102].

5.2. Ultrasonic Frequency

Ultrasonic frequency is also one of the main parameters in ultrasonic device. The microstructural properties (including grain sizes, phase composition, precipitated phase morphology, bonding interface, and porosity) and mechanical properties (including microhardness, wear rate, and elastic modulus) of parts at different levels of ultrasonic frequencies (0, 25, 33, and 41 kHz) were investigated.

As shown in Figure 9, the grains grew along the building direction with the columnar shape without ultrasonic vibration, while the grains demonstrated uniform distribution and equiaxed shapes with uniform grain boundaries.

However, as shown in Figure 6. The porosity value first decreased after introducing ultrasonic vibration with a frequency of 25 kHz and then increasing the ultrasonic frequency from 25 to 41 kHz. As a result, it is easy to remove the material from the part and then increase wear rate. The elastic modulus was decreased when ultrasonic frequency was increased from 25 to 41 kHz. The change in porosity might play an important role in the change in elastic modulus of the parts. In other words, ultrasonic frequency has a great influence on the microstructural properties, and there is an optimal range of ultrasonic frequency.

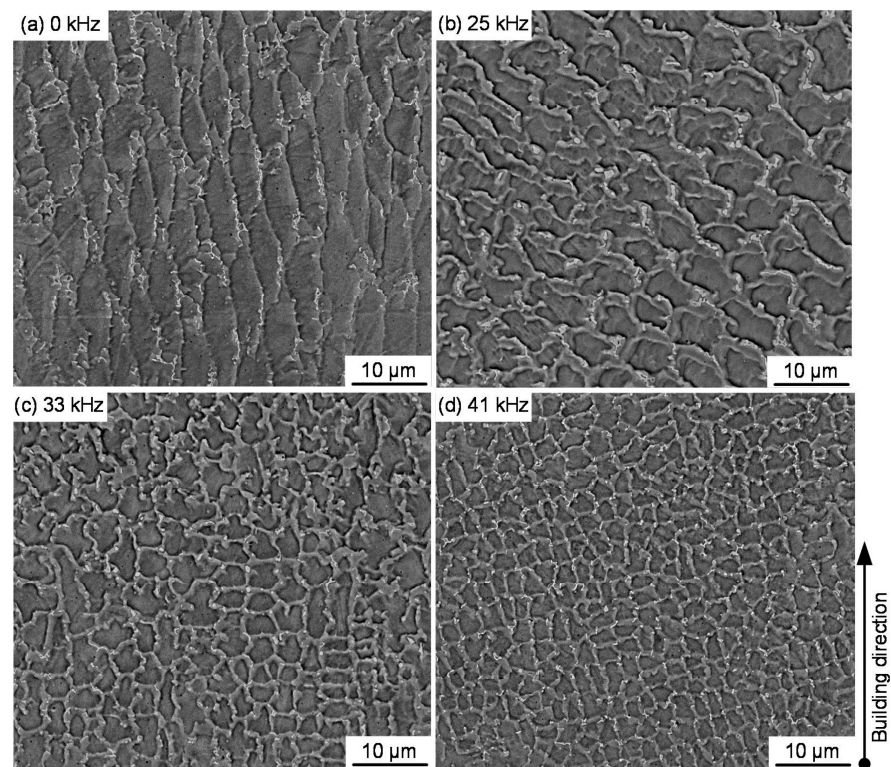


Figure 9. Effect of different ultrasonic frequencies on microstructures and grain sizes: (a) 0; (b) 25; (c) 33; (d) 41 kHz, reproduced or adapted from [43], with permission from Elsevier, 2020.

5.3. Ultrasonic Impact Scanning Speed

The top of the sample without ultrasonic impact treatment showed flaky, large, and skeletal columnar crystals, as shown in Figure 10a. By reducing the ultrasonic impact scanning speed and breaking the dendrites, grain refinement was more obvious. When the ultrasonic scanning speed was 6 mm/s, compared with the untreated top arc area, the microstructure mainly developed columnar crystals; some grains were refined, and the columnar crystals were large and not completely broken into sheets, as shown in Figure 10b. When the scanning speed was 4 mm/s, some columnar crystals were interrupted, and the grains were transformed into equiaxed grains, as shown in Figure 10c. When the scanning speed was 2 mm/s, the degree of refinement further increased, as shown in Figure 10d [103].

5.4. Ultrasonic Impact Times

Figure 11 shows the internal pores of a 2219 aluminum alloy manufactured by arc additive manufacturing without ultrasonic impact treatment and with treatment applied once, twice, and three times. The 2219 aluminum alloy without ultrasonic impact treatment contained many micron pores. There were fewer pores in the samples treated by the ultrasonic impact, the pores were extruded into an oval shape, and the tiny pores were closed. The statistical data of porosity number, average diameter, porosity, and porosity roundness (the ratio of the short axis to the long axis) of different UIT samples are shown in Table 4. After one ultrasonic impact, the number of stomata in the sample decreased by 13.2% compared with the non-ultrasonic impact treatment, and the average diameter decreased by 17.1%. After two ultrasonic impacts, the number of pores in the sample decreased by 20.4%, and the average diameter decreased by 13 μm compared with the non-ultrasonic impact treatment. After three ultrasonic impacts, the average pore diameter decreased to less than 20 μm , and the pore roundness was 0.66 [104].

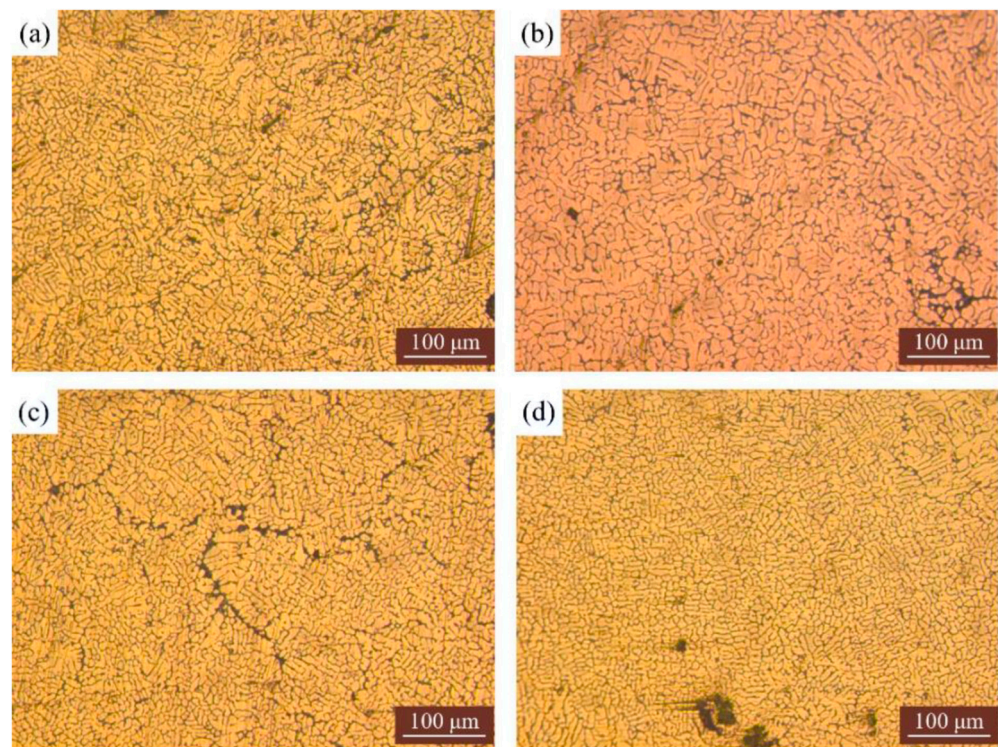


Figure 10. Microstructure of the arc area on the top of the additive sample with the different ultrasonic peening scanning speeds: (a) no ultrasonic impact; (b) 6 mm/s; (c) 4 mm/s; (d) 2 mm/s, reproduced or adapted from [81], with permission from MDPI, 2022.

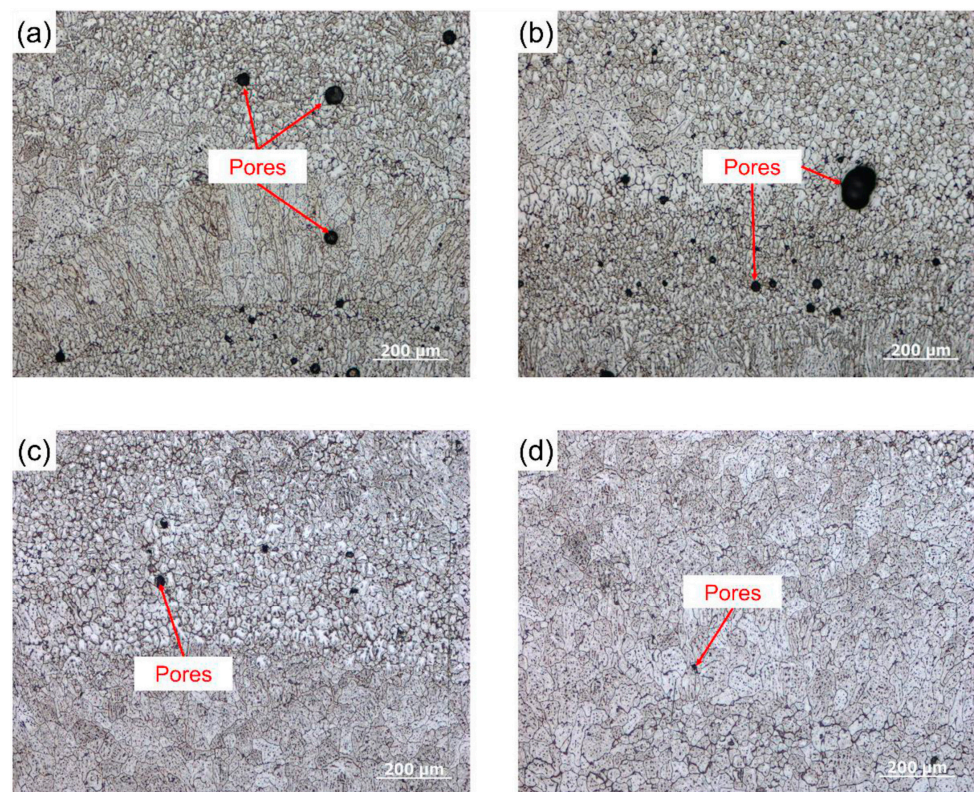


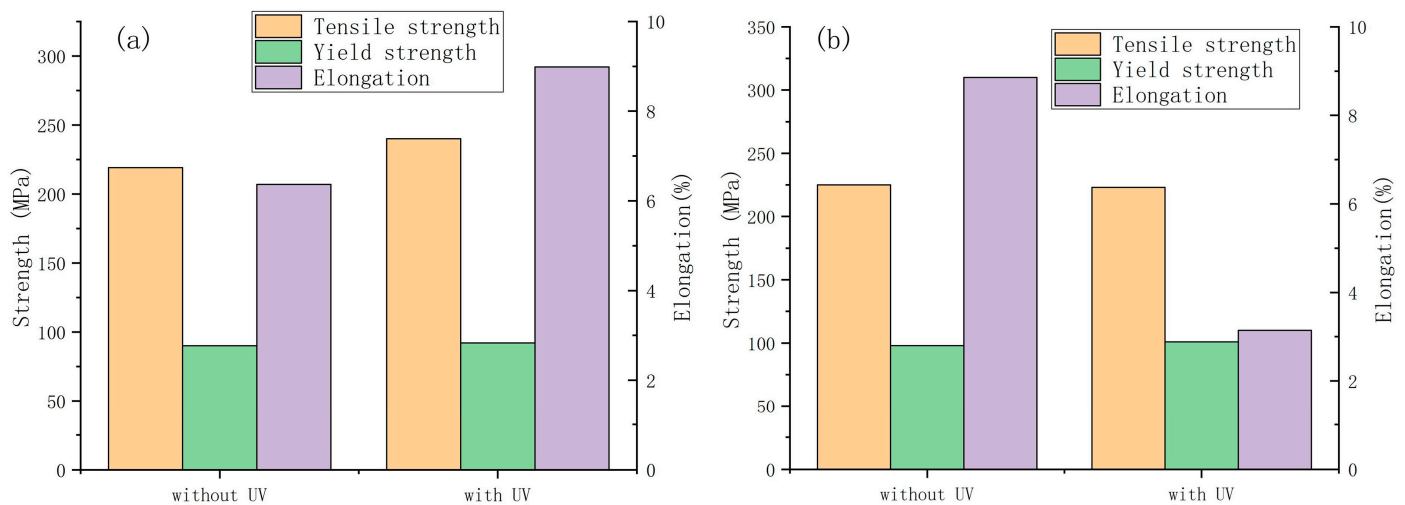
Figure 11. Pores in the samples with the different interlayered ultrasonic peening times: (a) no ultrasonic peening; (b) ultrasonic peening once; (c) ultrasonic peening twice; (d) ultrasonic peening three times, reproduced or adapted from [105], with permission from Elsevier, 2022.

Table 4. Pores of samples with the different interlayered ultrasonic peening times [81].

Index/Number of Ultrasonic Peening Treatments	None	One	Two	Three
Number of stomata	986	856	785	679
Average diameter/ μm	41	34	28	19
Porosity ratio/%	0.95	0.83	0.78	0.62
Porosity roundness	0.86	0.75	0.71	0.66

5.5. Action Direction of Ultrasonic Vibration

The tensile test results of the single-channel and multi-layer deposited parts are shown in Figure 12. The tensile strength, yield strength, and elongation of the 2319 aluminum alloy deposits assisted by ultrasonic vibration in the vertical direction were strengthened, and the tensile strength, yield strength, and elongation were improved. Among them, the tensile strength increased by about 8.61%, the yield strength increased by 3.44%, and the elongation increased by about 40.51%. This was mainly due to the grain refinement caused by additional ultrasonic vibration. However, when the yield strength of the 2319 aluminum alloy deposits assisted by ultrasonic vibration in the horizontal direction was increased, the elongation decreased significantly. The reason for this phenomenon may be that there are many porosity defects in the horizontal drawing parts with additional ultrasonic vibration, which leads to stress concentration in the process of tension, resulting in brittle fracture of the drawing parts [106].

**Figure 12.** Tensile test results of single-channel multilayer deposition samples: (a) horizontal direction; (b) vertical direction.

6. Conclusions

The WAAM process has the advantages of high material utilization and deposition efficiency, low production cost, and highly versatile equipment, so it has broad application prospects in the rapid prototyping of large and complex light alloy components in the aerospace field. However, because of the limitations of the high heat input, large residual stress, relatively low forming accuracy, and surface roughness in the manufacturing process, this process is still far from large-scale production and application. Other conclusions drawn from this review are:

- Ultrasonic assistance has been continuously combined with WAAM to consolidate large-size continuous materials and rapid precision manufacturing ability, which can effectively improve the microstructure and mechanical properties.
- Ultrasonic-assisted process parameters (such as ultrasonic amplitude, application direction, and impact times) have an intuitive effect on the product materials. In order

to improve the mechanical properties of WAAM product components, each parameter must be accurately set during the ultrasonic-assisted WAAM process.

7. Overview

The comprehensive optimization system of ultrasonic-assisted process parameters is not perfect. WAAM components have limitations such as large residual stress and low forming accuracy, which make them unsuitable for large-scale production in the aerospace field. In future research, in order to improve the ultrasonic-assisted process parameter optimization system, it will be necessary to analyze the effects of process parameters such as ultrasonic amplitude and the scanning speed on the average grain size of WAAM components and establish an algorithm to optimize the parameters with process parameters as factors. This is an important research direction to realize the further development of arc-fuse additive-manufacturing accuracy and defect control.

Author Contributions: Conceptualization, methodology, writing—first draft, Y.C. and Y.Z.; literature review, W.M. and J.M.; funding acquisition, Y.C. and W.H. All authors have read and agreed to the published version of the manuscript.

Funding: This work was supported by the Henan Provincial Youth Backbone University Teacher Training Plan (2021GGJS090) and Henan Provincial Key Development Project (22111240200).

Institutional Review Board Statement: Not applicable.

Informed Consent Statement: Not applicable.

Conflicts of Interest: The authors declare no conflict of interest.

References

1. Ding, J.; Colegrove, P.; Mehnen, J.; Ganguly, S.; Almeida, P.M.S.; Wang, F.; Williams, S. Thermo-mechanical analysis of Wire and Arc Additive Layer Manufacturing process on large multi-layer parts. *Comput. Mater. Sci.* **2011**, *50*, 3315–3322. [[CrossRef](#)]
2. Zalameda, J.N.; Burke, E.R.; Hafley, R.A.; Taming, K.M.B.; Domack, C.S.; Brewer, A.; Martin, R.E. Thermal Imaging for Assessment of Electron-Beam Freeform Fabrication (EBF3) Additive Manufacturing Deposits. In Proceedings of the Conference on Thermosense—Thermal Infrared Applications XXXV, Baltimore, MD, USA, 30 April–1 May 2013.
3. King, D.; Tansey, T. Rapid tooling: Selective laser sintering injection tooling. *J. Mater. Process. Technol.* **2003**, *132*, 42–48. [[CrossRef](#)]
4. Levy, G.N.; Schindel, R.; Kruth, J.P. Rapid manufacturing and rapid tooling with layer manufacturing (LM) technologies, state of the art and future perspectives. *Cirp Ann. Manuf. Technol.* **2003**, *52*, 589–609. [[CrossRef](#)]
5. Lu, B.; Li, D.; Tian, X. Development Trends in Additive Manufacturing and 3D Printing. *Engineering* **2015**, *1*, 85–89. [[CrossRef](#)]
6. Wong, K.V.; Hernandez, A. A review of additive manufacturing. *Int. Sch. Res. Not.* **2012**, *2012*, 208760. [[CrossRef](#)]
7. Frazier, W.E. Metal additive manufacturing: A review. *J. Mater. Eng. Perform.* **2014**, *23*, 1917–1928. [[CrossRef](#)]
8. Vayre, B.; Vignat, F.; Villeneuve, F. Designing for additive manufacturing. *Procedia CirP* **2012**, *3*, 632–637. [[CrossRef](#)]
9. Herzog, D.; Seyda, V.; Wycisk, E.; Emmelmann, C. Additive manufacturing of metals. *Acta Mater.* **2016**, *117*, 371–392. [[CrossRef](#)]
10. Milewski, J.O. *Additive Manufacturing of Metals*; Springer International Publishing AG: Cham, Switzerland, 2017.
11. Armstrong, M.; Mehrabi, H.; Naveed, N. An overview of modern metal additive manufacturing technology. *J. Manuf. Process.* **2022**, *84*, 1001–1029. [[CrossRef](#)]
12. Ramkumar, P.L.; Rijwani, T. Additive manufacturing of metals and ceramics using hybrid fused filament fabrication. *J. Braz. Soc. Mech. Sci. Eng.* **2022**, *44*, 455. [[CrossRef](#)]
13. Li, Y.; Su, C.; Zhu, J.J. Comprehensive review of wire arc additive manufacturing: Hardware system, physical process, monitoring, property characterization, application and future prospects. *Results Eng.* **2022**, *13*, 100330. [[CrossRef](#)]
14. Liu, J.; Dong, S.; Sun, C.; Zhang, Z.; Xu, B. Research status of quality control of direct energy deposition forming technology. *Manuf. Technol. Mach. Tools* **2020**, *6*, 44–48.
15. Wohlers, T.; Gornet, T. History of additive manufacturing. *Wohlers Rep.* **2014**, *24*, 118.
16. Gao, W.; Zhang, Y.B.; Ramanujan, D.; Ramani, K.; Chen, Y.; Williams, C.B.; Wang, C.C.L.; Shin, Y.C.; Zhang, S.; Zavattieri, P.D. The status, challenges, and future of additive manufacturing in engineering. *Comput. Aided Des.* **2015**, *69*, 65–89. [[CrossRef](#)]
17. Singh, S.; Ramakrishna, S.; Singh, R. Material issues in additive manufacturing: A review. *J. Manuf. Process.* **2017**, *25*, 185–200. [[CrossRef](#)]
18. Eskin, G.I. *Ultrasonic Treatment of Light Alloy Melts*; CRC Press: Boca Raton, FL, USA, 1998.
19. Babamiri, B.B.; Indeck, J.; Demeneghi, G.; Cuadra, J.; Hazeli, K. Quantification of porosity and microstructure and their effect on quasi-static and dynamic behavior of additively manufactured Inconel 718. *Addit. Manuf.* **2020**, *34*, 101380. [[CrossRef](#)]
20. Li, F.; Qi, B.J.; Zhang, Y.X.; Guo, W.; Peng, P.; Zhang, H.P.; He, G.Z.; Zhu, D.Z.; Yan, J.F. Effects of Heat Treatments on Microstructures and Mechanical Properties of Ti6Al4V Alloy Produced by Laser Solid Forming. *Metals* **2021**, *11*, 346. [[CrossRef](#)]

21. Paul, C.; Jinoop, A.; Bindra, K. Metal additive manufacturing using lasers. *Addit. Manuf. Appl. Innov.* **2018**, *57*, 37–94.
22. Wang, F.; Tzanakis, I.; Eskin, D.; Mi, J.; Connolley, T. In situ observation of ultrasonic cavitation-induced fragmentation of the primary crystals formed in Al alloys. *Ultrason. Sonochemistry* **2017**, *39*, 66–76. [[CrossRef](#)]
23. Bidare, P.; Jimenez, A.; Hassanin, H.; Essa, K. Porosity, cracks, and mechanical properties of additively manufactured tooling alloys: A review. *Adv. Manuf.* **2022**, *10*, 175–204. [[CrossRef](#)]
24. Long, P. *Study on Microstructure and Properties of 316 L Stainless Steel Produced by Arc Fuse*; Huazhong University of Science and Technology: Hangzhou, China, 2020. [[CrossRef](#)]
25. Sharma, S.K.; Grewal, H.S.; Saxena, K.K.; Mohammed, K.A.; Prakash, C.; Davim, J.P.; Buddhi, D.; Raju, R.; Mohan, D.G.; Tomkow, J. Advancements in the Additive Manufacturing of Magnesium and Aluminum Alloys through Laser-Based Approach. *Materials* **2022**, *15*, 8122. [[CrossRef](#)]
26. Raut, L.P.; Taiwade, R.V. Wire Arc Additive Manufacturing: A Comprehensive Review and Research Directions. *J. Mater. Eng. Perform.* **2021**, *30*, 4768–4791. [[CrossRef](#)]
27. Li, Z.W.; Xu, Z.W.; Ma, L.; Wang, S.; Liu, X.S.; Yan, J.C. Cavitation at filler metal/substrate interface during ultrasonic-assisted soldering. Part II: Cavitation erosion effect. *Ultrason. Sonochemistry* **2019**, *50*, 278–288. [[CrossRef](#)] [[PubMed](#)]
28. Wang, B.; Tan, D.Y.; Lee, T.L.; Khong, J.C.; Wang, F.; Eskin, D.; Connolley, T.; Fezzaa, K.; Mi, J.W. Data and videos for ultrafast synchrotron X-ray imaging studies of metal solidification under ultrasound. *Data Brief* **2018**, *17*, 837–841. [[CrossRef](#)]
29. Han, C.J.; Fang, Q.H.; Shi, Y.S.; Tor, S.B.; Chua, C.K.; Zhou, K. Recent Advances on High-Entropy Alloys for 3D Printing. *Adv. Mater.* **2020**, *32*, e1903855. [[CrossRef](#)]
30. Gu, D.D.; Ma, C.L.; Dai, D.H.; Yang, J.K.; Lin, K.J.; Zhang, H.M.; Zhang, H. Additively manufacturing-enabled hierarchical NiTi-based shape memory alloys with high strength and toughness. *Virtual Phys. Prototyp.* **2021**, *16*, S19–S38. [[CrossRef](#)]
31. Cooke, S.; Ahmadi, K.; Willerth, S.; Herring, R. Metal additive manufacturing: Technology, metallurgy and modelling. *J. Manuf. Process.* **2020**, *57*, 978–1003. [[CrossRef](#)]
32. Cunningham, C.R.; Flynn, J.M.; Shokrani, A.; Dhokia, V.; Newman, S.T. Invited review article: Strategies and processes for high quality wire arc additive manufacturing. *Addit. Manuf.* **2018**, *22*, 672–686. [[CrossRef](#)]
33. Zhang, D.Z.; Li, Y.Z.; Wang, H.; Cong, W.L. Ultrasonic vibration-assisted laser directed energy deposition in-situ synthesis of NiTi alloys: Effects on microstructure and mechanical properties. *J. Manuf. Process.* **2020**, *60*, 328–339. [[CrossRef](#)]
34. Chen, Y.H.; Xu, M.F.; Zhang, T.M.; Xie, J.L.; Wei, K.; Wang, S.L.; Yin, L.M.; He, P. Grain refinement and mechanical properties improvement of Inconel 625 alloy fabricated by ultrasonic-assisted wire and arc additive manufacturing. *J. Alloys Compd.* **2022**, *910*, 164957. [[CrossRef](#)]
35. Diao, M.X.; Guo, C.H.; Sun, Q.F.; Jiang, F.C.; Li, L.Y.; Li, J.F.; Xu, D.; Liu, C.M.; Song, H.L. Improving mechanical properties of austenitic stainless steel by the grain refinement in wire and arc additive manufacturing assisted with ultrasonic impact treatment. *Mater. Sci. Eng. A Struct. Mater. Prop. Microstruct. Process.* **2022**, *857*, 144044. [[CrossRef](#)]
36. Kumar, S.; Wu, C.S.; Padhy, G.K.; Ding, W. Application of ultrasonic vibrations in welding and metal processing: A status review. *J. Manuf. Process.* **2017**, *26*, 295–322. [[CrossRef](#)]
37. Xu, M.; Chen, Y.; Zhang, T.; Xie, J.; Wei, K.; Wang, S.; Yin, L. Effect of post-heat treatment on microstructure and mechanical properties of nickel-based superalloy fabricated by ultrasonic-assisted wire arc additive manufacturing. *Mater. Sci. Eng. A* **2023**, *863*, 144548. [[CrossRef](#)]
38. Wu, W.Z.; Li, J.L.; Jiang, J.L.; Liu, Q.P.; Zheng, A.D.; Zhang, Z.; Zhao, J.; Ren, L.Q.; Li, G.W. Influence Mechanism of Ultrasonic Vibration Substrate on Strengthening the Mechanical Properties of Fused Deposition Modeling. *Polymers* **2022**, *14*, 904. [[CrossRef](#)] [[PubMed](#)]
39. Li, G.X.; Bie, W.B.; Zhao, B.; Chen, F.; Zhao, C.Y.; Zhang, Y.M. Ultrasonic assisted machining of gears with enhanced fatigue resistance: A comprehensive review. *Adv. Mech. Eng.* **2022**, *14*, 57. [[CrossRef](#)]
40. Shu, S.; Guo, J.X.; Liu, X.L.; Wang, X.J.; Yin, H.Q.; Luo, D.M. Effects of pore sizes and oxygen-containing functional groups on desulfurization activity of Fe/NAC prepared by ultrasonic-assisted impregnation. *Appl. Surf. Sci.* **2016**, *360*, 684–692. [[CrossRef](#)]
41. Yi, Z.Y.; Song, C.C.; Zhang, G.H.; Tong, T.Q.; Ma, G.Y.; Wu, D.J. Microstructure and Wear Property of ZrO₂-Added NiCrAlY Prepared by Ultrasonic-Assisted Direct Laser Deposition. *Materials* **2021**, *14*, 5785. [[CrossRef](#)]
42. Nový, F.; Petru, M.; Trško, L.; Jambor, M.; Bokůvka, O.; Lago, J. Fatigue Properties of Welded Strenx 700 MC HSLA Steel after Ultrasonic Impact Treatment Application. *Mater. Today Proc.* **2020**, *32*, 174–178. [[CrossRef](#)]
43. Wang, H.; Hu, Y.B.; Ning, F.D.; Cong, W.L. Ultrasonic vibration-assisted laser engineered net shaping of Inconel 718 parts: Effects of ultrasonic frequency on microstructural and mechanical properties. *J. Mater. Process. Technol.* **2020**, *276*, 116395. [[CrossRef](#)]
44. Williams, S.W.; Martina, F.; Addison, A.C.; Ding, J.; Pardal, G.; Colegrove, P. Wire plus Arc Additive Manufacturing. *Mater. Sci. Technol.* **2016**, *32*, 641–647. [[CrossRef](#)]
45. Uralde, V.; Veiga, F.; Aldalur, E.; Suarez, A.; Ballesteros, T. Symmetry and Its Application in Metal Additive Manufacturing (MAM). *Symmetry* **2022**, *14*, 1810. [[CrossRef](#)]
46. Liu, J.N.; Xu, Y.L.; Ge, Y.; Hou, Z.; Chen, S.B. Wire and arc additive manufacturing of metal components: A review of recent research developments. *Int. J. Adv. Manuf. Technol.* **2020**, *111*, 149–198. [[CrossRef](#)]
47. Wang, T.T.; Zhang, Y.B.; Xie, Y.L. Research status and prospect of wire arc additive manufacturing technology. *Electr. Weld.* **2017**, *47*, 5.

48. Xiong, J.; Zhang, G.J. Adaptive control of deposited height in GMAW-based layer additive manufacturing. *J. Mater. Process. Technol.* **2014**, *214*, 962–968. [[CrossRef](#)]
49. Tamayo, J.A.; Riascos, M.; Vargas, C.A.; Baena, L.M. Additive manufacturing of Ti6Al4V alloy via electron beam melting for the development of implants for the biomedical industry. *Heliyon* **2021**, *7*, e06892. [[CrossRef](#)] [[PubMed](#)]
50. Mahmoud, D.; Magolon, M.; Boer, J.; Elbestawi, M.A.; Mohammadi, M.G. Applications of Machine Learning in Process Monitoring and Controls of L-PBF Additive Manufacturing: A Review. *Appl. Sci.* **2021**, *11*, 11910. [[CrossRef](#)]
51. An, N.Y.; Shuai, S.S.; Hu, T.; Chen, C.Y.; Wang, J.; Ren, Z.M. Application of Synchrotron X-Ray Imaging and Diffraction in Additive Manufacturing: A Review. *Acta Metall. Sin. Engl. Lett.* **2022**, *35*, 25–48. [[CrossRef](#)]
52. Wu, B.T.; Pan, Z.X.; Ding, D.H.; Cuiuri, D.; Li, H.J.; Xu, J.; Norrish, J. A review of the wire arc additive manufacturing of metals: Properties, defects and quality improvement. *J. Manuf. Process.* **2018**, *35*, 127–139. [[CrossRef](#)]
53. Kobayashi, M.; Dorce, Y.; Toda, H.; Horikawa, H. Effect of local volume fraction of microporosity on tensile properties in Al-Si-Mg cast alloy. *Mater. Sci. Technol.* **2010**, *26*, 962–967. [[CrossRef](#)]
54. Yi, J.; Guan, G.; Li, S.K.; Liu, Z.W.; Gong, Y.L. Effect of post-weld heat treatment on microstructure and mechanical properties of welded joints of 6061-T6 aluminum alloy. *Trans. Nonferrous Met. Soc. China* **2019**, *29*, 2035–2046. [[CrossRef](#)]
55. Zhang, J.K.; Chen, B.H.; Zhang, X. Residual stress at the interface of titanium alloy produced by arc addition and its effect. *Rare Met. Mater. Eng.* **2018**, *47*, 7.
56. Chi, J.; Cai, Z.; Wan, Z.; Zhang, H.; Chen, Z.; Li, L.; Li, Y.; Peng, P.; Guo, W. Effects of heat treatment combined with laser shock peening on wire and arc additive manufactured Ti17 titanium alloy: Microstructures, residual stress and mechanical properties. *Surf. Coat. Technol.* **2020**, *396*, 125908. [[CrossRef](#)]
57. Dinovitzer, M.; Chen, X.H.; Laliberte, J.; Huang, X.; Frei, H. Effect of wire and arc additive manufacturing (WAAM) process parameters on bead geometry and microstructure. *Addit. Manuf.* **2019**, *26*, 138–146. [[CrossRef](#)]
58. Veiga, F.; Suarez, A.; Aldalur, E.; Artaza, T. Wire arc additive manufacturing of invar parts: Bead geometry and melt pool monitoring. *Measurement* **2022**, *189*, 110452. [[CrossRef](#)]
59. Mukhanov, I.; Golubev, Y.M. Strengthening Steel Components by Ultrasonically Vibrating Ball. *Vestn. Mashinostr.* **1966**, *11*, 52–53.
60. Statnikov, E.S.; Korolkov, O.V.; Vityazev, V.N. Physics and Mechanism of Ultrasonic Impact. *Ultrasonics* **2006**, *44*, e533–e538. [[CrossRef](#)]
61. Campbell, J. Effects of vibration during solidification. *Int. Met. Rev.* **1981**, *26*, 71–108. [[CrossRef](#)]
62. Jian, X.; Xu, H.; Meek, T.T. Effect of power ultrasound on solidification of aluminum A356 alloy. *Mater. Lett.* **2005**, *59*, 190–193. [[CrossRef](#)]
63. Cong, W.; Ning, F. A fundamental investigation on ultrasonic vibration-assisted laser engineered net shaping of stainless steel. *Int. J. Mach. Tools Manuf.* **2017**, *121*, 61–69. [[CrossRef](#)]
64. Chen, C.Y.; Deng, Q.L.; Song, J.L. Effect of ultrasonic vibration on laser cladding process. *Electromach. Die* **2005**, *3*, 4.
65. Chen, C.Y.; Deng, Q.L.; Song, J.L. Effect of Ni content and ultrasonic vibration on cracks in laser cladding. *J. Nanjing Univ. Aeronaut. Astronaut.* **2005**, *37*, 5.
66. Qin, L.Y.; Wang, W.; Yang, G. Experimental study on ultrasonic-assisted laser deposition of titanium alloy. *China Laser* **2013**, *40*, 0103001.
67. Wang, T.; Zhang, A.F.; Liang, S.D.; Yan, S.P.; Zhang, L.Z.; Li, D.C. Study on as-deposited microstructure and properties of IN718 by ultrasonic vibration-assisted laser metal forming. *China Laser* **2016**, *43*, 6.
68. Wang, T.; Zhang, A.F.; Zhang, W.L.; Liang, S.D.; Li, S.; Yan, S.P.; Zhang, L.Z. Research progress of ultrasonic vibration-assisted laser metal forming technology. *Appl. Laser* **2015**, *35*, 4.
69. Koli, Y.; Yuvaraj, N.; Aravindan, S. Enhancement of Mechanical Properties of 6061/6082 Dissimilar Aluminium Alloys Through Ultrasonic-Assisted Cold Metal Transfer Welding. *Arab. J. Sci. Eng.* **2021**, *46*, 12089–12104. [[CrossRef](#)]
70. Yuan, D.; Shao, S.Q.; Guo, C.H.; Jiang, F.C.; Wang, J.D. Grain refining of Ti-6Al-4V alloy fabricated by laser and wire additive manufacturing assisted with ultrasonic vibration. *Ultrason. Sonochemistry* **2021**, *73*, 105472. [[CrossRef](#)] [[PubMed](#)]
71. Malaki, M.; Ding, H. A Review of Ultrasonic Peening Treatment. *Mater. Des.* **2015**, *87*, 1072–1086. [[CrossRef](#)]
72. Krylov, N.A.; Polischuk, A.M. The use of ultrasonic equipment for metal structure stabilization. *Basic Phys. Ind. Ultrason. Appl. Part* **1970**, *1*, 70.
73. Khurshid, M.; Leitner, M.; Barsoum, Z.; Schneider, C. Residual stress state induced by high frequency mechanical impact treatment in different steel grades—Numerical and experimental study. *Int. J. Mech. Sci.* **2017**, *123*, 34–42. [[CrossRef](#)]
74. Ma, Q.S.; Chen, H.Z.; Ren, N.N.; Zhang, Y.Y.; Hu, L.; Meng, W.; Yin, X.H. Effects of Ultrasonic Vibration on Microstructure, Mechanical Properties, and Fracture Mode of Inconel 625 Parts Fabricated by Cold Metal Transfer Arc Additive Manufacturing. *J. Mater. Eng. Perform.* **2021**, *30*, 6808–6820. [[CrossRef](#)]
75. Roy, S.; Fisher, J.W.; Yen, B.T. Fatigue resistance of welded details enhanced by ultrasonic impact treatment (UIT). *Int. J. Fatigue* **2003**, *25*, 1239–1247. [[CrossRef](#)]
76. Mordyuk, B.N.; Prokopenk, G.I.; Vasylyev, M.A.; Iefimov, M.O. Effect of structure evolution induced by ultrasonic peening on the corrosion behavior of AISI-321 stainless steel. *Mater. Sci. Eng. A Struct. Mater. Prop. Microstruct. Process.* **2007**, *458*, 253–261. [[CrossRef](#)]

77. Yang, Y.C.; Jin, X.; Liu, C.M.; Xiao, M.Z.; Lu, J.P.; Fan, H.L.; Ma, S.Y. Residual Stress, Mechanical Properties, and Grain Morphology of Ti-6Al-4V Alloy Produced by Ultrasonic Impact Treatment Assisted Wire and Arc Additive Manufacturing. *Metals* **2018**, *8*, 934. [[CrossRef](#)]
78. Cheng, X.H.; Fisher, J.W.; Prask, H.J.; Gnaupel-Herold, T.; Yen, B.T.; Roy, S. Residual stress modification by post-weld treatment and its beneficial effect on fatigue strength of welded structures. *Int. J. Fatigue* **2003**, *25*, 1259–1269. [[CrossRef](#)]
79. Rao, D.L.; Chen, L.G.; Ni, C.Z.; Zhu, Z.Q. Effect of ultrasonic impact on residual stress of welded structure. *Weld. J.* **2005**, *26*, 4.
80. Mordyuk, B.N.; Karasevskaya, O.P.; Prokopenko, G.I.; Khripta, N.I. Ultrafine-grained textured surface layer on Zr-1%Nb alloy produced by ultrasonic impact peening for enhanced corrosion resistance. *Surf. Coat. Technol.* **2012**, *210*, 54–61. [[CrossRef](#)]
81. Zhang, J.; Xing, Y.F.; Zhang, J.J.; Cao, J.Y.; Yang, F.Y.; Zhang, X.B. Effects of In-Process Ultrasonic Vibration on Weld Formation and Grain Size of Wire and Arc Additive Manufactured Parts. *Materials* **2022**, *15*, 5168. [[CrossRef](#)] [[PubMed](#)]
82. Yang, D.Q.; Wang, X.W.; Peng, Y.; Zhou, Q.; Wang, K.H. Study on Microstructure and Properties of 316L stainless Steel produced by Ultrasonic impact assisted Melt Arc addition. *Mater. Guide* **2022**, *1*, 122–125.
83. Zhang, Y.-Z.; Wang, Z.-G.; Xie, L.-Y.; Ding, Z.-Y.; Ma, Y.-H.; Ouyang, J.-H.; Liu, Z.-G.; Wang, Y.-J.; Wang, Y.-M. Laser surface nanocrystallization of oxide ceramics with eutectic composition: A comprehensive review. *Heat Treat. Surf. Eng.* **2021**, *3*, 37–54. [[CrossRef](#)]
84. Ye, X.L.; You, Z.L.; Kan, W. Effects of Ultrasonic Impact Treatment on the Residual Stress and Fatigue Performance of Ultrahigh Strength Steel Weld Joint. In Proceedings of the International Technology and Innovation Conference 2006, Hangzhou, China, 6–7 November 2006; pp. 150–154. [[CrossRef](#)]
85. Abdullah, A.; Malaki, M.; Eskandari, A. Strength enhancement of the welded structures by ultrasonic peening. *Mater. Des.* **2012**, *38*, 7–18. [[CrossRef](#)]
86. Xiao, C.H. *Study on the Elimination of Welding Residual Stress and Deformation by Real-Time Ultrasonic Impact*; Harbin Institute of Technology: Harbin, China, 2013.
87. Gao, H.; Dutta, R.K.; Huizenga, R.M.; Amirthalingam, M.; Hermans, M.J.M.; Buslaps, T.; Richardson, I.M. Stress relaxation due to ultrasonic impact treatment on multi-pass welds. *Sci. Technol. Weld. Join.* **2014**, *19*, 505–513. [[CrossRef](#)]
88. Shao, Z.W.; Le, Q.C.; Zhang, Z.Q.; Cui, J.Z. Effect of ultrasonic power on grain refinement and purification processing of AZ80 alloy by ultrasonic treatment. *Met. Mater. Int.* **2012**, *18*, 209–215. [[CrossRef](#)]
89. Wang, D.P.; Song, N.X.; Wang, T.; Huo, L.X. Nano-treatment of ultrasonic metal surface. *J. Tianjin Univ.* **2007**, *40*, 6.
90. Hu, G.F.; Yang, Y.; Sun, R.; Qi, K.; Lu, X.; Li, J.D. Microstructure and properties of laser cladding NiCrBSi coating assisted by electromagnetic-ultrasonic compound field. *Surf. Coat. Technol.* **2020**, *404*, 126469. [[CrossRef](#)]
91. Xu, J.L.; Zhou, J.Z.; Tan, W.S.; Huang, S.; Wang, S.T.; He, W.Y. Ultrasonic vibration on wear property of laser cladding Fe-based coating. *Surf. Eng.* **2020**, *36*, 1261–1269. [[CrossRef](#)]
92. Wen, X.; Cui, X.F.; Jin, G.; Zhang, X.R.; Zhang, Y.; Zhang, D.; Fang, Y.C. Design and characterization of FeCrCoAlMn_{0.5}Mo_{0.1} high-entropy alloy coating by ultrasonic assisted laser cladding. *J. Alloys Compd.* **2020**, *835*, 155449. [[CrossRef](#)]
93. Yang, Y.T.; Zhang, Y.Y.; Yu, W. Study on the properties of titanium alloy welded joints treated by ultrasonic impact treatment. *Mater. Dev. Appl.* **2007**, *22*, 5.
94. Zhao, X.H.; Wang, D.P.; Wang, X.B.; Deng, C.Y.; Zu, Z.Q. Loading ultrasonic impact improves the fatigue performance of TC4 titanium alloy welded joints. *J. Weld.* **2010**, *11*, 4.
95. Haagenen, P.J.; Statnikov, E.S.; Lopez-Martinez, L. Introductory fatigue tests on welded joints in high strength steel and aluminium improved by various methods including ultrasonic impact treatment (UIT). *IIW Doc* **1998**, *13*, 1748–1798.
96. Yang, X.; Zhou, J.; Ling, X. Study on plastic damage of AISI 304 stainless steel induced by ultrasonic impact treatment. *Mater. Des. (1980–2015)* **2012**, *36*, 477–481. [[CrossRef](#)]
97. He, Z.; Hu, Y.; Qu, H.; Wang, Z.M.; Bu, X.Z. Study on the anisotropy of titanium alloy parts fabricated by ultrasonic impact arc. *Aerosp. Manuf. Technol.* **2016**, *6*, 6.
98. Xu, M.F.; Chen, Y.H.; Deng, H.B.; Ji, D. Study on Microstructure and Mechanical Properties of TC4 Titanium Alloy produced by Ultrasonic assisted CMT Arc addition. *Precis. Form. Eng.* **2019**, *5*, 7.
99. Chen, W.; Chen, Y.; Zhang, T.; Wen, T.; Yin, Z.; Feng, X. Effect of ultrasonic vibration and interpass temperature on microstructure and mechanical properties of Cu-8Al-2Ni-2Fe-2Mn alloy fabricated by wire arc additive manufacturing. *Metals* **2020**, *10*, 215. [[CrossRef](#)]
100. Yuan, D.; Sun, X.; Sun, L.; Zhang, Z.; Guo, C.; Wang, J.; Jiang, F. Improvement of the grain structure and mechanical properties of austenitic stainless steel fabricated by laser and wire additive manufacturing assisted with ultrasonic vibration. *Mater. Sci. Eng. A* **2021**, *813*, 141177. [[CrossRef](#)]
101. Ming, W.; Guo, X.; Xu, Y.; Zhang, G.; Jiang, Z.; Li, Y.; Li, X. Progress in Non-Traditional Machining of Amorphous Alloys. *Ceram. Int.* **2023**, *49*, 1585–1604. [[CrossRef](#)]
102. Zhang, Z.; Zhang, Y.; Liu, D.; Zhang, Y.; Zhao, J.; Zhang, G. Bubble behavior and its effect on surface integrity in laser-induced plasma micro-machining silicon wafer. *ASME J. Manuf. Sci. Eng.* **2022**, *144*, 091008. [[CrossRef](#)]
103. Zhou, C. *Study on Temperature Field and Stress Field of Laser Metal Deposition Assisted by Ultrasonic Impact*; Harbin University of Engineering: Harbin, China, 2021; p. 000087.
104. Wu, Y.; Deng, W.; Liu, K.; Zhang, Z.; Wu, D.; Chen, M.; Bai, J. Effect of interlaminar ultrasonic impact on microstructure and mechanical properties of 2219 aluminum alloy produced by TIG arc addition. *Aviat. Sci. Technol.* **2021**, *32*, 80–86.

105. Wang, C.; Li, Y.; Tian, W.; Hu, J.; Li, B.; Li, P.; Liao, W. Influence of ultrasonic impact treatment and working current on microstructure and mechanical properties of 2219 aluminium alloy wire arc additive manufacturing parts. *J. Mater. Res. Technol.* **2022**, *21*, 781–797. [[CrossRef](#)]
106. Li, P.; Guo, S.; Yang, D.; Peng, Y.; Yan, D.; Li, D.; Wang, K. Ultrasonic vibration assisted arc augmentation Material manufacturing 2219 aluminum alloy structure and mechanical properties [J/OL]. *China J. Nonferrous Met.* **2022**, *1*, 1–12. Available online: <https://kns.cnki.net/kcms/detail/43.1238.TG.20220919.1009.002.html> (accessed on 19 September 2022).

Disclaimer/Publisher’s Note: The statements, opinions and data contained in all publications are solely those of the individual author(s) and contributor(s) and not of MDPI and/or the editor(s). MDPI and/or the editor(s) disclaim responsibility for any injury to people or property resulting from any ideas, methods, instructions or products referred to in the content.